PROTEINS: Structure, Function, and Genetics 33:119–134 (1998)

Molecular Dynamics Simulations of Human Carbonic Anhydrase II: Insight Into Experimental Results and the Role of Solvation

Dongsheng Lu and Gregory A. Voth*
Department of Chemistry and Henry Eyring Center for Theoretical Chemistry, University of Utah, Salt Lake City, Utah

ABSTRACT **In this paper, the carbonic anhydrase II (CA II) enzyme active site is modeled using ab initio calculations and molecular dynamics simulations to examine a number of important issues for the enzyme function. It is found that the Zn^{2+} ion is dominantly tetrahedrally coordinated, which agrees with X-ray crystallographic studies. However, a transient five-fold coordination with an extra water molecule is also found. Studies of His64 conformations upon a change in the protonation states of the Zn-bound water and the His64 residue also confirm the results of an X-ray study which suggest that the His64 conformation is quite flexible. However, the degree of water solvation is found to affect this behavior. Water bridge formation between the Zn-bound water and the His64 residue was found to involve a free energy barrier of 2–3 kcal/mol and an average lifetime of several picoseconds, which supports the concept of a proton transfer mechanism through such a bridge. Mutations of various residues around the active site provide further insight into the corresponding experimental results and, in fact, suggest an important role for the solvent water molecules in the CA II catalytic mechanism. Proteins 33:119–134, 1998.** © 1998 Wiley-Liss, Inc.

Key words: molecular modeling; proton transfer; enzyme catalysis; mutations; molecular mechanics

INTRODUCTION

Carbonic anhydrase II (CA II) is one of the most efficient enzymes that has ever been studied experimentally.[1,2] This enzyme catalyzes the interconversion between CO_2 and HCO_3^- with a turnover rate $10^6\ s^{-1}$. The overall reaction is

$$CO_2 + H_2O \rightleftharpoons H^+ + HCO_3^-, \qquad (1)$$

which is of physiological importance in the transport of CO_2 in the human body as well as in plants.

The structure of CA II has been extensively characterized by X-ray experiments.[3–8] It consists of a single polypeptide chain of 260 residues with molecular weight of about 30 kDa.[9] The enzyme active site cavity is about 15 Å wide and 15 Å deep, with a zinc ion residing at the bottom of the cavity. The Zn^{2+} ion is coordinated by three histidine residues, His94, 96, and 119, whose major biological importance is to constrain the Zn^{2+} ion in the active site. Mutation of any of these residues leads to much larger zinc dissociation constant and around a 1000-fold decrease in catalytic power.[10]

It has been consistently found in X-ray experiments that at most one water molecule is closely bound to the Zn^{2+} ion, which then forms a close to tetrahedral coordination geometry, together with the three histidine groups. However, from these experiments one cannot completely exclude the possible presence of a water molecule which might transiently adopt a fifth ligand position around the Zn^{2+} ion, since in the enzyme crystal some water molecules may be difficult to detect experimentally—and there may be fewer of them—than in the fully solvated state. As described later, this effect can be illustrated from simple computer simulation studies where water molecules are added to fully solvate the X-ray structure. In the X-ray structure, there are only 7–10 water molecules detected within a distance of 10 Å from the Zn^{2+} ion in the active site, while there can be as many as 20 water molecules when it is fully solvated in the simulations. In the X-ray structures of Nair et al.[3] at two pH conditions, pH = 5.7 and 6.5, the closest water molecules were found to be 2.7 and 2.6 Å away from the Zn^{2+} ion, respectively; while in the mutation variant H119C,[11] the nearest water was 3.5 Å away from the Zn^{2+} ion. This is interesting because the Zn-water affinity is very large, on the order of 30–40 kcal/mol. It should be noted that there is not any theoretical evidence from first-principles calculations to support the 4-fold coordination picture, but it seems intuitively obvious and therefore has been used as a guide for molecular

Grant sponsor: National Institutes of Health; Grant number: 1RO1-GM-53148.
*Correspondence to: Gregory A. Voth, Department of Chemistry, University of Utah, Salt Lake City, UT 84112. E-mail: voth@chemistry.chem.utah.edu
Received 19 February 1998; Accepted 7 May 1998

TABLE I. The Experimental Results for a Number of Mutation Studies, Which Are Taken From Reference 15

Variant	k_{cat}/K_M ($\mu M^{-1}\ s^{-1}$)	pK_a	zinc K_d (pM)
Wild type	110	6.8	4
H94D	0.11	≥9.6	15000
H94C	0.11	≥9.5	33000
T199D	0.04		4
T199E	0.04		0.02
Q92A	29	6.8	18
Q92N	27	6.9	5
Q92E	12	7.7	5
E117A	19	6.9	40
E117Q	0.002	≥9.9	4400

modeling of the active site[12,13] based on the experimental X-ray results.

There have also been extensive catalytic activity studies carried out on CA II.[2,10,14–22] These studies have been the foundation of the generally accepted catalytic mechanism underlying Equation 1, which consists of two steps. First, a proton is transferred from the Zn-bound water (pK_a around 7) to a residue, thought to be His64, thus generating a Zn-bound hydroxide. This proton is subsequently transferred to buffer or solvent. After the generation of the hydroxide ion, it is attacked by CO_2, in the process of which a bicarbonate ion forms and leaves the active site. At high buffer concentrations, the proton transfer from the Zn-bound water to His64 is the rate-limiting step in the overall process. At low buffer concentrations, the release of the proton from His64 to the solvent becomes rate-limiting.[17,18]

Some of the most useful experimental information comes from mutations of various residues. Mutation of His64 with other residues under various conditions[16,23] has suggested that the proton transfer from the Zn-bound water to His64 is the pathway which leads to the high catalytic activity. This result has led to the first example of structure-based design of intramolecular proton transfer in CA V.[24,25] It is also interesting that the X-ray crystallographic studies[3] have found that the conformation of His64 is sensitive to the pH conditions. However, from the X-ray structural data alone, it was not clear as to the cause of the shift in the conformations.

Indirect ligands of the Zn^{2+} ion, such as Q92 and E117, also have biological importance by constraining the directly bound His94 and His119 ligands: His-94 donates a hydrogen bond (H-bond) to the carboxiamide side chain of Q92, while His119 donates a hydrogen bond to the carboxylate side chain of Glu117. Upon mutation of these residues,[21,22] the catalytic activity decreases (See Table I), revealing the fact that the active site ligands have been optimally selected by Nature, as one might expect. Under extreme mutations such as E117Q, the zinc dissociation constant increases significantly, and the variant shows little catalytic activity. Yet, the X-ray crystallographic studies of wild type CA II and the variant E117Q show that they are isostructural.[15] In this case, a H-bond scheme which assumes deprotonation of His-119 has been proposed to explain the decrease of catalytic power.[15] However, this suggestion may be questioned considering the large energy barrier likely involved in such a deprotonation. Moreover, it may contradict the observed increase of the zinc dissociation constant upon mutation, since the formation of a deprotonated H119 anion should bind more tightly to the Zn^{2+} ion, potentially leading to a decrease in the dissociation constant through electrostatic considerations. On the other hand, the pK_a of the Zn-bound water is observed to increase. Thus, a completely satisfactory explanation for the effects of some of the mutations may not yet exist.

Other mutations have focused on residues such as Thr199 which are indirectly involved in the catalytic process. This case is very interesting in the sense that mutation of this residue leads to a decrease of k_{cat}/K_M by 1000- to more than 5000-fold,[26,27] even much larger than the cases where direct histidine ligands are mutated. The microscopic origin of this effect remains to be revealed.

It should be noted that while X-ray experiments have been shown to be invaluable in exploring the structures of enzymes and providing understanding on possible enzyme mechanisms,[4–8] they have limitations intrinsic to the experimental method itself. In the crystalline state, an enzyme may have fewer and less mobile water molecules in the active site, and only those water molecules which are relatively static can be identified in the X-ray experiments without ambiguity. Thus, the crystallographic data may lack the solvent and solvation information which can be important to the chemical process of interest. For example, information about the structure and free energy of formation of *transient* water configurations between the Zn-bound water and the His64 residue cannot be obtained from X-ray data, yet this dynamical information may be crucial for an understanding of the mechanism of proton transfer. As was discussed above, several site-specific mutagenesis studies may also not be satisfactorily explained from the X-ray results alone. Thus, other routes must be explored, e.g., computer simulations as in the present paper, in order to achieve a more complete understanding of the enzyme function.

One of the key difficulties in molecular dynamics computer simulation often comes from the lack of an accurate model. Because of the incomplete transferability of potential energy models between different types of physical systems of interest, there is not likely to be a universal model that will work in all systems, at least for some subdomains of the various systems. As purely quantum simulations are still

beyond the reach of present computer power despite the efforts toward this direction,[28] more empirical modeling of the CA II active site is therefore necessary in order to obtain results from molecular dynamics computer simulations.

The usual empirical approach to modeling biophysical systems relies on a combination of theoretical ab initio calculations and fitting to experimentally determined properties. Depending on the properties of interest, different models may be obtained. In the present study, models for the forward and backward proton transfer situations in CA II will be developed based primarily on ab initio results. With this model, a number of important issues are examined, including the number of water ligands around the Zn^{2+} ion, the conformation of the His64 residue upon a change in the protonation state of the Zn-bound water and His64, the probability and average lifetime of water bridge formation between the Zn-bound water and the His64 residue, and some mutation studies of direct ligands, indirect ligands, and the Thr199 residue. The solvent effects on the structure and dynamics of the protein residues are also explored. By virtue of this approach, it is also shown that computer simulations and X-ray experiments provide two complementary tools for exploring the behavior of the CA II enzyme.

This paper is organized in the following manner: First, the empirical interaction models are developed which are then used in the MD simulations; the MD simulation methodology is also discussed. The results of the simulation and discussions of a number of issues are then presented and concluding remarks are given in the final section.

MODEL DEVELOPMENT AND SIMULATION METHODOLOGY

Since the ligands around the Zn^{2+} ion in CA II directly affect the pK_a of the Zn-bound water, and this in turn further affects the catalytic mechanism, the behavior of a second water molecule around the Zn^{2+} ion may be crucial to understanding the enzyme function. Intuitively, one would expect that the water association around the Zn^{2+} ion is a result of zinc-water affinities. If the $Zn^{2+}(Im)_3(H_2O)$ complex has a significant affinity for a second water ligand, then this water molecule may be more closely bound around the Zn^{2+} site than other waters in the active site; conversely, if this affinity is small, then there will be little association of the second water to the Zn^{2+} ion. In the present study, an empirical model will be fit first to ab initio and experimental frequency results, and then second to ab initio water affinities.

The first and second water affinities for the $Zn^{2+}(Im)_3$ complex which corresponds to the association reactions (2) and (3) below were calculated to be 35.1 and 18.3 kcal/mol, respectively:

$$(Im)_3Zn^{2+} + H_2O \rightleftharpoons (Im)_3Zn^{2+}(H_2O), \quad (2)$$

$$(Im)_3Zn^{2+}(H_2O) + H_2O \rightleftharpoons (Im)_3Zn^{2+}(H_2O)_2, \quad (3)$$

where "Im" stands for an imidazole molecule. The calculation method is the same as used in our previous ab initio study,[29] namely RHF/3-21G geometry optimizations with MP2/4-31G* energy calculations. This method has been shown to reproduce a number of reactions and conformational barriers with reasonable accuracy. All of the ab initio calculations were carried out using the Gaussian94 program.

In the present model, a normal harmonic force has been employed for the Zn-His ligand interactions, except for the cases where the direct ligands were mutated. For the latter case, a Morse type potential was instead used in order to give the Zn-His bond the capability of dissociation. The various parameters obtained after fitting to the calculated water affinities are presented in Table II. The charges of the

TABLE II. The Parameters of the CA II Model†

Nonbonded parameters		
Atom	R^*	ϵ
Zn	1.0	0.014
OZ	1.768	0.152
NZ	1.85	0.2
Bond parameters		
Bond type	r_{eq}, Å	k_r, kcal/(mol Å^2)
Zn-NZ	2.04	40.0
Zn-OZ	1.85	94.0
OZ-HZ	0.957	540.0
Zn-OT(Morse)	2.06	
Angle parameters		
Angle type	θ_{eq}, deg	k_θ, kcal/(mol rad^2)
NZ-Zn-NZ	109.5	23.0
NZ-Zn-OZ/OT	109.5	23.0
CE-NZ-Zn	126.0	20.0
CD-NZ-Zn	126.0	20.0
Zn-OZ/OT-H	124.0	20.0
Morse parameters		
Bond type	D_M (kcal/mol)	μ (Å^{-1})
Zn-OT	13.0	0.4
Zn-NZ	80.0	0.58

†The Morse potential for Zn-NZ is only used in the direct ligand mutant simulations, while the other parameters are used consistently in all other simulations. OZ: the Zn-bound hydroxide oxygen atom when Zn-bound water is deprotonated; OT: Zn-bound water oxygen; NZ: the nitrogen atom directly bound to the Zn^{2+} ion (NE2 atoms in His94 and His96, ND1 atom in His119) (See Fig. 1).

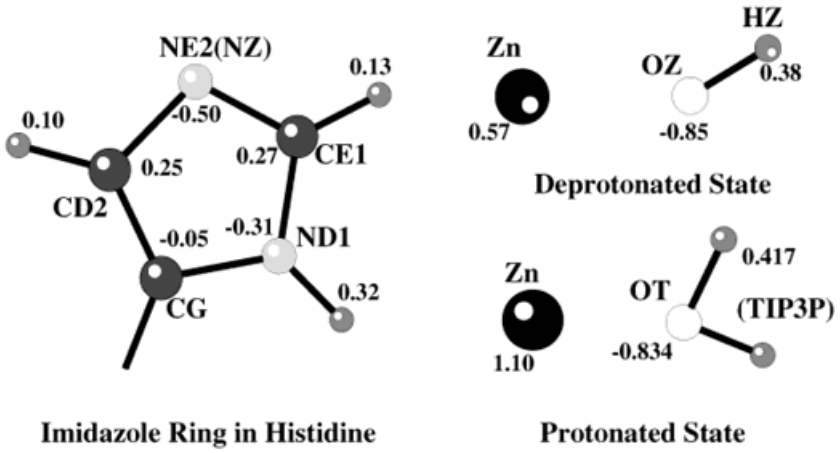

Fig. 1. The charge distribution of the imidazole rings, zinc ion, and Zn-bound water/hydroxide used in the present model. The charges were obtained from ab initio calculations with the Merz/Kollman algorithm[30] and then modified later to fit the ab initio water affinities.

active site complex were initially obtained from ab initio calculations by the Merz/Kollman algorithm,[30,31] and then modified to yield the desired water affinities (Fig. 1). The same charge distribution was used for the imidazole ring of the His-ligands for both protonation states of the Zn-bound water.

The harmonic force constant for the Zn-NZ interactions (the reader is referred to Figure 1 for atomic type definitions) was chosen to be 40 kcal/(mol Å^2) based on experimental frequency data,[12] and an equilibrium distance of 2.04 Å was used as obtained from ab initio calculations. For the Zn-OT interaction, a Morse potential with well depth of 13.0 kcal/mol, equilibrium distance 2.06 Å and exponent 0.4 Å^{-1} was imposed in addition to the non-bonding interaction (Table II) in order to get the best fit to the ab initio geometry and first water affinity of $Zn^{2+}(Im)_3$ complex to be around 35 kcal/mol. The angular interaction of NZ-Zn-NZ among the histidine ligands and NZ-Zn-O were harmonically parametrized to be 23 kcal/(mol rad^2) as a result of ab initio calculations and fitting to the second water affinity of the $Zn^{2+}(Im)_3$ complex. Here "O" stands for either OT or OZ atoms in Figure 1. This procedure will be described in more detail when the results on the number of water molecules around the Zn^{2+} ion are discussed.

As Zn-bound water is deprotonated, the complex $Zn^{2+}(Im)_3(OH^-)$ has a calculated water affinity around 12.2 kcal/mol. In the same way, the parameters for the backward proton transfer configuration were chosen and fitted to the water affinity (See Table II). The ESP charge (Fig. 1) for Zn from ab initio (RHF/4-31G*) calculations was about 0.73 electron charge but lowered to 0.57 in order to obtain a more accurate water affinity. The angular interaction parameters were retained from the Zn-bound water case.

For the Morse type Zn-L model used in direct ligand mutations, the potential well depth for the Zn-His interaction was fitted to the ab initio result for imidazole binding, which is around 84 kcal/mol for the reaction

$$(Im)_2Zn^{2+} + Im \rightleftharpoons (Im)_3Zn^{2+}. \quad (4)$$

After including the pure electrostatic interaction between the Zn^{2+} ion and the imidazole rings, and after redistribution of charges, the Morse potential well was around 90 kcal/mol. The exponent μ was then found to be 0.67 Å^{-1} after a fit to a harmonic potential well with a force constant 40.0 kcal/(mol Å^2) as described before, in which $\mu = (k/D_M)^{1/2}$ was used. This model will be discussed further when the results on the direct ligand mutations are described.

Version 23 of the CHARMM program[32] was used for all the classical MD simulations. The program was modified to include the Morse type potentials between the atoms as needed. Except for the parameters presented in Table II for the active site binding, all the other parameters for bonds, angles, dihedrals, etc., among protein atoms and solvent molecules were from the CHARMM23 parameter set. The solvent water molecules were represented by the TIP3P water model.[33] A 13 Å cutoff was used for the nonbonded interactions, which was updated every 25 time steps. The extended model was used for the electrostatic interactions to generate a long-range fluctuating, rather than static, electric field.[34,35] The latter has been shown to lead to an increased damping of atomic fluctuations. In the study of Stote et al,[36] it was found that long-range electrostatic interactions are important for maintaining the correct geometry of zinc binding site when using a non-bonded model for the zinc-protein interactions.

The CA II coordinates were originally obtained from the Brookhaven protein data bank. The enzyme was solvated with 210 waters around the active site. The water molecules were kept within a 28 Å sphere around the zinc ion by the use of a harmonic restraining force [0.5 kcal/(mol Å^2)], which was applied to any water molecule that strayed out of the sphere. Minimization was performed by using the ABNR minimization routine implemented in the CHARMM program.[32] The original geometry of the protein was constrained with a 1.0 kcal/(mol Å^2) harmonic potential, and the constraints were released step by step afterwards. Mutations of specific residues were carried out by cutting site chain atoms and generating new atoms according to the specified geometry which gives a good fit to the X-ray structures. Then hydrogen atoms were generated by the HBUILD utility in CHARMM program[32] and geometry optimization was performed before the MD simulations. Each MD simulation consisted of at least a 40 ps equilibration run and a 40 ps production run with a timestep 1.0 fs.

RESULTS AND DISCUSSION

Number of Water Molecules Around Zinc: One or Two?

The number of direct water ligands around zinc was a subject of discussion in some of the early work on CA.[37,38] In this section, results of the MD simulations are presented and discussed which focus on the issue of how close the second water ligand residues are from the zinc center.

The most straightforward case is for the backward proton transfer situation where Zn-bound water is deprotonated. Here, a consistent 4-fold coordination picture is found around the Zn ion from the MD simulations. This is satisfactorily explained by the small Zn-complex affinity for the fifth water, which is only around 12.2 kcal/mol. This number is not much more than the hydrogen-bonding interaction between water molecules. In addition, the association of a second water molecule to the Zn^{2+} ion will cost considerable entropy which is another factor favoring the tetrahedrally coordinated Zn^{2+} ion in this case.

The forward proton transfer situation is somewhat more subtle. In the MD simulations, both 4- and 5-fold coordinated zinc can be achieved through changes in the angular interaction for NZ-Zn-NZ and NZ-Zn-OT. By defining the direct ligands as those which are within 2.4 Å from the Zn^{2+} ion, it is seen in Table III that the coordination number changes upon changing the NZ-Zn-NZ and NZ-Zn-OT bending force constants. When k_θ is smaller than 10 kcal/(mol rad^2), the Zn^{2+} ion is 5-fold coordinated. As the force constant is increased above 30 kcal/(mol rad^2), the second water is virtually excluded from the direct ligand position. This result is not unexpected: by increasing the force constant for NZ-Zn-NZ and NZ-Zn-OT, the tetrahedrally coordinated ligand positions become more rigid, so the second water cannot as easily distort the other ligands to occupy a fifth ligand position.

TABLE III. The Change of Zinc Coordination Upon Changing Force Constant of NZ-Zn-NZ and NZ-Zn-O†

$k_{NZ–Zn–NZ}$	$k_{NZ–Zn–O}$	Percent of 4-fold coordination
30	30	≥99%
23	23	~92%
20	20	~85–90%
15	15	~70–80%
10	10	≤2%
5	5	~0%

†"O" stands for OZ or OT which is directly bound to the Zn^{2+} ion in Figure 1. The equilibrium angles were set at 109.5° and the units of the force constant are kcal/(mol rad^2). The water is taken to be a ligand to Zn when R(Zn-O) is less than 2.4 Å.

To help resolve the issue of the angular force constant, ab initio calculations were carried out on the $Zn^{2+}(Im)_3(H_2O)$ complex with the Zn-NZ distance fixed at 2.10 Å, which is consistent with the experimental X-ray value. Then, the potential energy surface was obtained as a function of the NZ-Zn-NZ angles. The calculation method is the same as described in our previous ab initio studies.[29] The resulting harmonic bending force constant was determined to be around 20–26 kcal/(mol rad^2) with an estimate of error to be within 6–8 kcal/mol.

The Zn-NZ bond stretching force constant also indirectly influences the average Zn-NZ distances in the simulations. This will in turn affect the angular force constant, since the repulsion among the histidine/imidazole ligands will decrease as they are further away from the Zn^{2+} ion. As will be discussed later in the direct ligand mutation studies, the value of 40 kcal/(mol Å^2) may be slightly too high, while another model based on the statistical methods by Vedani et al.[39] may be more realistic. Depending on the coordination of the Zn^{2+} ion, an effective stretching force constant from 28 to 35 kcal/(mol Å^2) may be more reasonable, but there is not enough evidence to support its use at this time. However, if this force constant is used for the Zn-NZ bonds, the average Zn-NZ bond length is found to increase from 2.11–2.12 to 2.14–2.15 Å. This would then lead to a slight decrease in the angular force constant from that described in the previous paragraph. The constraining force from the protein residues may also have an effect on the angular interactions. This latter effect is rather hard to quantify because of the complexity of protein environment, but it is expected to be not more than 5 kcal/mol since the repulsive force comes mainly from the overlap of electron clouds of the neighboring NZ atoms.

TABLE IV. The Change of His64 Conformation and the Zn-bound Histidine Ligands Upon Changing the Protonation States of Zn-bound Water and His64 in the MD Simulations†

Zn-bound water	His64	R(Zn-NE2)	R(Zn-CA)	R(Zn-His94)	R(Zn-His96)	R(Zn-His119)
Protonated	Deprotonated	7.6	8.2	2.09	2.11	2.15
Protonated	Protonated	12.5	10.1	2.11	2.10	2.14
Deprotonated	Protonated	13.0	9.9	2.14	2.13	2.19
Deprotonated	Deprotonated	11.3	9.7	2.13	2.12	2.18
X-ray pH = 5.7		11.1	9.9	2.3	2.1	2.3
X-ray pH = 6.5		7.2/11.6	10.0/10.0	2.5	2.3	2.5
X-ray pH = 8.5		7.6	9.9	2.0	2.1	1.9

†Here "NE2" and "CA" atoms are in the His64 residue. The X-ray experimental results from Reference 3 are also shown for comparison. Notice both "inward" and "outward" conformations were observed at pH = 6.5. The units are in Å.

From the above arguments, the effective angular force constant is most likely to be around 18–28 kcal/(mol rad^2). In the present study, a mean value of 23 kcal/(mol rad^2) was used, since it is consistent with the above arguments and approximately reproduces the ab initio calculated second water affinity for $Zn^{2+}(Im)_3$ complex at zero temperature when it is combined with the charge distribution in Figure 1. To be more specific, the second water affinities are 23.7, 19.4, 18.5, and less than 17 kcal/mol for angular force constants of 10, 20, 23 and 30 kcal/(mol rad^2), respectively. Hence, the choice of 23 kcal/(mol rad^2) approximately reproduces the general binding properties of the water molecules and gives a picture of a dominantly 4-fold coordinated Zn^{2+} ion, which is consistent with a number of X-ray studies.[3,5–8]

It is worth noting that the 5-fold coordinated Zn-complex in situations of small angular force constants tends to push the Thr199 away from the Zn-bound water, which also contradicts a number of experimental facts, especially the mutation studies which have established the importance of Thr199 in the catalytic mechanism. It was also observed when the angular force constant is smaller 5 kcal/(mol rad^2) that a water molecule from the back of the three histidines can attack the Zn^{2+} ion, which is considered to be quite unrealistic, as it was never found in X-ray crystallographic studies (Christianson, D.W., personal communication.)

From the above ab initio modeling and the resulting MD simulations, it was concluded that the Zn^{2+} ion is dominantly tetrahedrally coordinated regardless of the protonation state of the Zn-bound water, in agreement with the X-ray results. The transient 5-fold coordination with a second water molecule is identified only 8% of the time, and this transient behavior could not be observed in X-ray experiments. Even if one considers the possible errors involved in the calculations, one is still likely to reach a similar conclusion; the only difference might be a 10 to 15% increase in the 5-fold coordination. The existence of 5-fold coordinated ligand situation around the Zn^{2+} ion might be important to some relevant catalytic processes as suggested by Liang and Lipscomb.[38] It should be noted, however, that without a careful determination of the empirical parameters as in the present study, incorrect conclusions may be obtained from the simulations. In fact, using a totally non-bonded model, the coordination number of the Zn^{2+} will always be found to be five unless the Lennard-Jones parameters and the charge distribution are explicitly set to exclude the second water ligand away from the Zn^{2+} ion, leading to unrealistic values for these parameters in the model.

His64 Conformations

The most efficient pathway for proton transfer in CA II appears to involve His64 as a proton acceptor. It has been speculated that two water molecules between Zn-bound water and His64 may serve as a bridge which would allow the proton transfer to happen through a shuttle mechanism.[2] This speculation is based on the X-ray structures of CA II, where the distance between the Zn^{2+} ion and acceptor NE2 atom on His64 is around 7.9 Å.[5,6,8] Clearly this distance and the formation of a water bridge should be crucial to the rate of the proton transfer. Nair and Christianson[3] found in X-ray experiments that the conformation of His64 is rather flexible upon changing pH and mutation of some residues around the active site (in this case it was Thr200).[21] At high pH, His64 likes to stay in an "inward" conformation in which the NE2 atom of His64 is around 7–8 Å away from the Zn^{2+} ion; on the other hand, His64 prefers an "outward" conformation in which NE2 atom is around 11–12 Å away from the Zn^{2+} ion at low pH.

To explore the His64 conformation issue, MD simulations with different protonation states of Zn-bound water and His64 were carried out. The results from the simulations of these states confirm the fact that His64 indeed has flexible conformations. However, there are some interesting differences from the X-ray results. The relevant distances upon changing protonation states are given in Table IV for both the MD simulations and X-ray results. In the X-ray studies, at a high pH (8.5) condition, which would likely give a double deprotonated state for the Zn-bound water and the His64 residue, an "inward"

conformation was found; while in the MD simulations, His64 shows an "outward" state with an R(Zn-NE2) distance of around 11.3 Å. This difference may be due to the solvation of the active site in the latter case. Interestingly enough, the doubly deprotonated state in a MD simulation designed to mimic the X-ray structure (87 waters) gives an "inward" conformation, as opposed to the MD result for the fully solvated structure (210 waters). This result suggests that the His64 conformation is sensitive to the involvement of the water molecules. A shortage of H-bond formation with water molecules in the X-ray based structure may result in an "inward" conformation.

Another difference is that the "outward" conformations from simulations show situations in which the His64 is more distant from the Zn^{2+} ion than in the X-ray structures (See Table IV). Moreover, the whole His64 residue shifts "inward" and "outward;" while in the X-ray structures, the alpha carbon atom of His64 remains to be around 9.9 Å for all pH conditions. This may be again due to the involvement of solvent water molecules. Certainly, there are other factors that may be important for the His64 conformations, such as the protonation state of other residues, the involvement of an electrolyte medium, etc., which are all beyond the present considerations.

Despite the differences between the X-ray and fully solvated MD simulation results, the conformational change of His64 upon changing the pH condition can be primarily understood by the change of protonation state of the His64 residue, which causes a different electrostatic environment around the active site. One reason for the change may be due to the repulsion between the positive charge on the protonated His64 and the Zn^{2+} ion. The shift of conformations may also be attributed to the involvement of water molecules which are trying to solvated the protonated His64. It is conceivable that upon protonation, His64 tends to be fully solvated by the aqueous medium, which can be achieved by assuming "outward" conformations. In any case, the conformational change of His64 upon changing the protonation state implies its biological significance: such a change makes it easier for the delivery of proton to the solvent medium, as pointed out by Nair and Christianson.[3]

The Water Bridge Formation

The importance of a water bridge from the Zn-bound water to the His64 residue for the proton shuttle process and the catalytic mechanism is likely to be substantial. The free energy of the water bridge formation is thereby one of the major concerns of the present study, as was mentioned in the Introduction. It was observed in the MD simulations that there are two water molecules which form a bridge between the Zn-bound water and His64 NE2. A typical water bridge formation is shown in Figure 2. Here, it is

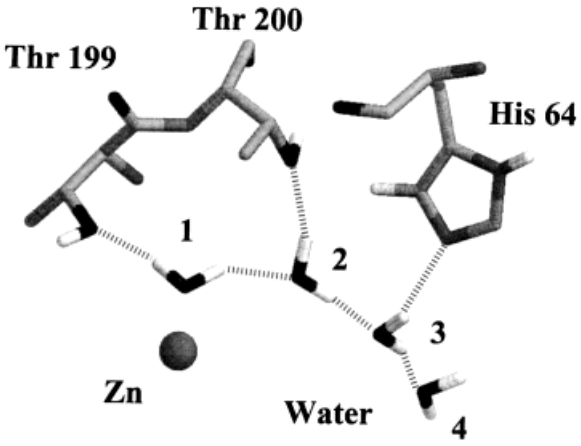

Fig. 2. A typical picture of the water bridge formation between the Zn-bound water (1) and His64.

observed that the Zn-bound water (water 1) donates H-bonds to water 2 and a Thr199 OG1 atom (not shown); water 2 donates H-bonds to waters 3 and 4; water 3 donates H-bonds to the His64 NE2 atom and the Thr200 OG atom. In the MD simulation, the bridge formation is defined by the three H-bonds among waters 1, 2, and 3 in Figure 2, which is simply a combination of distance criteria (R(OO) $\leq$ 3.3 Å) and angular criteria ($\angle$O-H-O $\geq$ 145°).

The free energy of bridge formation can be directly calculated from the simulations without any special sampling techniques. From a number of 50–100 ps simulation runs, the probability of forming a water bridge such as the one shown in Figure 2 was found to be around 1–4%, with an average bridge lifetime of about 1–4 picoseconds, which may be long enough for the proton shuttle to operate effectively. This probability of bridge formation corresponds to a free energy barrier of ~2–3 kcal/mol, as calculated from the expression

$$\Delta F = k_B T \ln \mathrm{P} \qquad (5)$$

in which "k_B" is Boltzmann's constant and "P" is the probability. It is interesting that the angular criterion is satisfied less frequently than the distance criterion in the simulations. Combining the calculated water bridge formation free energy with a barrier of ~8–10 kcal/mol for the first proton transfer from the Zn-bound water,[29] it seems that proton transfer from Zn-bound water to His64 mediated by a water bridge is quite feasible energetically. This result provides further theoretical support for the suggestion of a CA II proton transfer mechanism between Zn-bound water and His64.[23]

It should be mentioned that there are also some cases where only one water stays in between the Zn-bound water and the His64 NE2 atom. This kind of situation cannot be ruled out since the minimum

Fig. 3. The model system of a single water bridge formation. An imidazole has been used in place of Zn-bound water, which is supported by the argument of similar pK_a for these two groups/complex. See text for details.

distance between the Zn-bound water and the His64 NE2 atom can be as low as 5–6 Å. In fact, it was found that the bridge formation of a single water molecule between these two groups appeared as much as 0.5% of the time in the simulations, though the average lifetime of this configuration was about 1 ps. This is noteworthy since the proton transfer barrier through a single-water bridge can be much smaller than the two-water bridge. A model ab initio calculation of the proton transfer barrier between two imidazole molecules through a single water bridge (See Fig. 3) gives a barrier of less than a few kcal/mol when both N · · · O distances (Fig. 3) are optimized. Under a favorable H-bonding situation, the proton in the form of H_3O^+ may even be energetically favorable. This model system employing an imidazole molecule in place of the Zn-bound water may be justified by the fact that the two groups have similar pK_a values.

One interesting observation regarding the single water bridge scenario is that the PT barrier changes as the two N · · · O distances (Fig. 3) change, as might be expected. With both distances fixed at 2.8 Å, the proton transfer can be shown to be concerted with two minima, where the proton stays with either of the imidazole molecules. The barrier is around 3–4 kcal/mol. The consideration of N · · · O bond length fluctuations is important since it can be readily shown from simulations that a distance of 2.8 Å is typical of the single water bridge case, while the optimized geometry with N · · · O distances of 2.54 Å is rare.

The above results are therefore suggestive of a situation in which both single and double water bridges may be important to the proton transfer in CA II. Unfortunately, the structural data from X-ray experiments can not give a complete picture of the transient water bridge since the latter is not a static structure. Håkansson et al.'s X-ray structure[40] shows evidence of a double water bridge, but the N-O distance between the terminal water in the bridge and the His64 NE2 seems too large (3.22 Å) to facilitate efficient proton transfer through the chain.[29] Therefore, even more accurate MD simulations will be required in the future to provide further conclusive evidence, including the role of nuclear quantization and tunneling effects.

Mutation Studies

Direct ligands

Mutation of the direct ligands (H94, H96 and H119) of the Zn^{2+} ion affects the association of zinc around the active site.[15] For all the mutants that have been studied experimentally, the zinc dissociation constant increased by a factor of 3800 to 15000. At the same time, the CO_2 hydration rate was affected by a factor of 30 to more than 1000 (See Table I).

As discussed earlier, a Morse type potential was used in this case for the Zn-His interactions in order to give the capability of zinc dissociation. In addition, the charge transfer from Zn to the His-ligands in the wild type CA II model were redistributed in order to reflect the charge balance as Zn dissociates. Two mutants H94D and H94C were prepared by replacing the H94 residue with the explicit mutated residues (D or C). Then the configuration was equilibrated slowly for a few picoseconds with a harmonic force of 2 kcal/mol imposed on the active site residues, which diminished as time evolves. The resulting configuration was then used for the subsequent simulation studies. This harmonic force-constrained equilibration was necessary as some of the mutants can evolve abruptly into distinct structures or may diffuse away, which is not considered to be realistic.

The large dissociation constant of the Zn^{2+} ion in direct ligand mutants is inferred from the X-ray structure studies in that some of the mutants have zinc in them, while others do not. This suggests that a correct parameter set should give a signature of zinc dissociation upon direct ligand mutation, which would then provide some guidance for further refining the potential parameters. A series of parameter sets were used in the present study. The results for H94D are presented in Table V. Here it is observed that $\mu = 0.67$ Å^{-1} seems to be too high, since even with a Morse potential well with $D_M = 70$ kcal/mol for the Zn-NZ bond the Zn^{2+} ion does not show enough diffusion. This may suggest that the Zn-NZ bond stretching force constant of 40 kcal/(mol Å^2) used in the studies reported in the previous section may be slightly too high, which leads to a slightly too large value of μ. As D_M decreases from 100 kcal/mol to 60 kcal/mol, while keeping the value $\mu = 0.67$ Å^{-1} constant, the Zn^{2+} ion goes from rigid to more diffusive behavior. The maximum Zn-NZ distance can be as large as 2.9 Å, at which time the Zn^{2+} ion is not associated with the histidine ligands. Due to the

TABLE V. The Distance Between Zn and Glu94 OE, His96 NZ, and His119 NZ Atoms for Different Potential Parameters†

D_M (kcal/mol)	μ (Å^{-1})	R(Zn-Glu94 OE)	R(Zn-His96 NZ)	R(Zn-His119 NZ)
100.0	0.67	1.89 (1.79, 2.03)	2.15 (1.97, 2.20)	2.14 (1.96, 2.21)
90.0	0.67	1.87 (1.79, 2.01)	2.17 (1.99, 2.23)	2.15 (1.97, 2.25)
80.0	0.67	1.84 (1.77, 1.99)	2.19 (1.98, 2.28)	2.15 (2.01, 2.27)
70.0	0.67	1.81 (1.71, 1.93)	2.22 (2.01, 2.31)	2.20 (2.03, 2.38)
90.0	0.58	1.84 (1.78, 1.98)	2.19 (2.02, 2.28)	2.27 (2.03, 2.40)
80.0	0.58	1.78 (1.70, 1.89)	2.21 (2.01, 2.30)	2.37 (2.11, 2.70)
70.0	0.58	1.88 (1.76, 2.01)	2.38 (2.05, 2.91)	2.59 (2.20, 2.89)

†The number outside the parenthesis is the average distance, and the numbers inside the parenthesis are the minimum and maximum observed in simulation studies over a 60–80 ps period. The corresponding distance between Zn and His ligands for wild-type CA II is around 2.17 (1.98, 2.28) Å for D_M = 80.0 kcal/mol and μ = 0.58 Å^{-1}. An appropriate choice of D_M will be around 70 ~ 90 kcal/mol with μ = 0.58 Å^{-1}. The distances are in units of Å.

limitations on the length of MD runs for the present model, the Zn^{2+} ion could not be totally dissociated, solvated by water molecules, and then leave the active site. This may also be influenced by the Morse potential imposed between the Zn^{2+} ion and histidine ligands, and by the representation of the Zn-Glu94 interactions. It can be shown that the ab initio energy curve will go to the dissociation limit faster than the Morse potential curve used in simulations. The interaction between Zn and Glu94 is also strong enough that it will act to keep Zn^{2+} around the active site. After this extensive qualitative optimization, the Morse parameters were thus chosen to be D_M = 80–90 kcal/mol with μ = 0.58 which gives reasonable zinc dissociation behavior, though there is clearly a need for more refinement in the future.

With these parameters in hand, one can now turn to the structures of the mutants. In the case of the H94D mutant, the D94 residue experiences strong interactions with the Zn^{2+} ion. The Zn-OE bond in D94 is much stronger than the Zn-NZ bond because of the large partial charges on the OE atoms. Then one may raise the question here: Why does the Zn^{2+} ion in D94 mutant dissociate more easily than in wild-type CA II upon replacement by more strongly-bound ligand? A possible resolution of the issue can be found from the motions of the Zn^{2+} ion and its ligands in the dynamic picture: The D94 side chain is not as rigid as H94 side imidazole ring in wild-type CA II, and its side chain is not at the optimal position to constrain the Zn^{2+} ion, which means the binding of Zn-OE in the H94D mutant does not cooperate as well with the other two histidine groups (H94 and H119) as H94 does in wild-type CA II. As can be seen in Figure 4, the Zn^{2+} ion is pulled away some from His96 and His119 to Asp94, while there are usually two water molecules around the Zn^{2+} ion. As a result, more room is available for the water molecules to attack the Zn^{2+} ion, leading to a larger dissociation constant. Thus, it seems likely that the cooperation of the three histidines and their ability to hold the

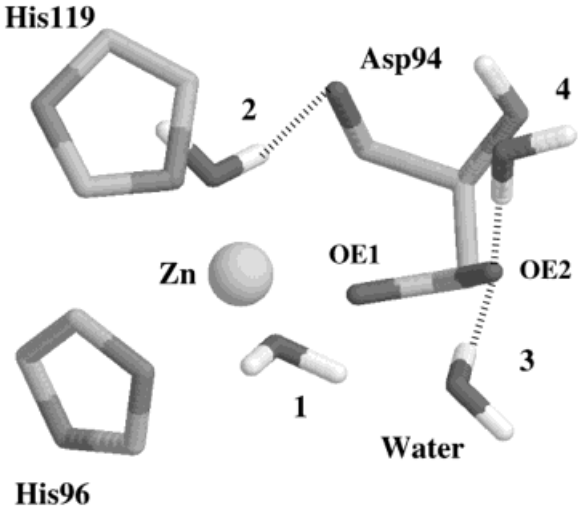

Fig. 4. The typical picture of mutant H94D found in the present MD simulations.

Zn^{2+} ion from the attack by water molecules is essential to the biological function of the enzyme. The similar conclusion was reached by Christianson and Fierke in X-ray and mutation studies.[15]

Mutant H94C was found in mutation experiments to be more complicated than mutant H94D in that the engineered enzyme can be the metal-bound or metal-free depending on the preparation of Cys side chain. When a negative charged thiolate side chain is used, the metal-bound enzyme is obtained. On the other hand, an air-oxidized C94 side chain crystallizes in a different space group and gives metal-free enzyme.[10,11] In the present work, mutants with both neutral and negatively charged Cys side chains were studied.

For the H94C mutant with a neutral C94 side chain, it was observed in the MD simulations that C94 drifted away from the Zn^{2+} ion, which was then replaced by two water molecules. This is expected since the charge on a SG atom in the CHARMM

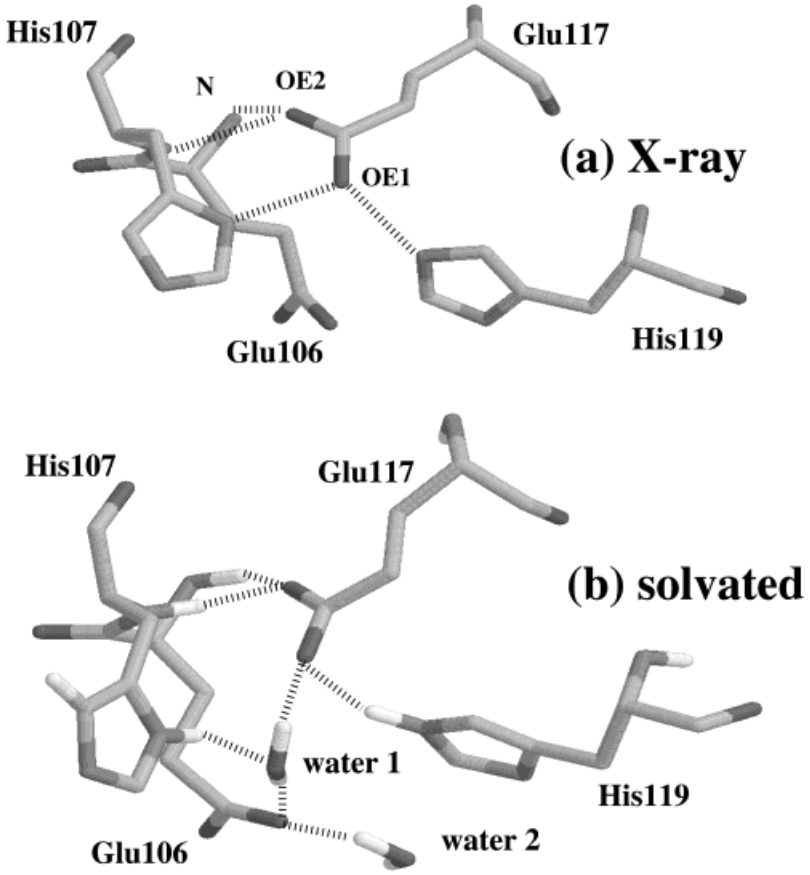

Fig. 5. **a:** The X-ray resolved structure of wild type CA II around the 117 residue region. Hydrogen atoms are not seen in the X-ray structures, and no water molecules were found close to this region. **b:** The corresponding picture when the X-ray structure in the upper panel is fully solvated. In the latter case, one water molecule is involved in the H-bonding in the region.

model is only −0.23 in the case of a neutral side chain. Thus it will not be able to effectively compete with the dipoles of water molecules. As there are three water molecules surrounding the Zn^{2+} ion in this case, the solvation and dissociation of zinc would then be much easier than in mutant H94D, where D94 can make significant contribution to the constraining of the Zn^{2+} ion through strong electrostatic interactions. It is very likely that in this case a metal-free variant will be observed in the experiments, as found by Alexander et al.[41] Unfortunately, this is very difficult to quantify in simulations without a more accurate model.

With a negative charged thiolate side chain, mutant H94C shows a ligand situation around the Zn^{2+} ion similar to what was found in H94D, where C94 side chain binds strongly with zinc, and there are two water molecules around the Zn^{2+} ion. Thus it is expected that this H94C mutant will give metal-bound enzyme and show zinc dissociation behavior similar to that of H94D, as found in experiments (See Table I).

Indirect ligands

The indirect ligands have been shown to have subtle effects on the catalytic behavior of the CA enzyme.[15,21] As was discussed in the Introduction, the mutations of E117, for example, lead to issues which are yet to be resolved. To explore this issue, studies of the E117Q and E117A variants were carried out in the MD simulations.

Before discussing the mutated variants, it is informative to examine the H-bond formation around residue 117 in wild type CA II. A typical picture for the solvated structure is presented in Figure 5(b) along with the X-ray determined structure in Figure 5(a). Generally, these two structures are quite similar in terms of the H-bonding, except the involvement of water molecules in the solvated structures. For example, in both structures, one OE (OE2) atom of E117 accepts two H-bonds from backbone E106 and H107 N atoms, meanwhile another OE (OE1) atom accepts a H-bond from the H119 NE2 atom. The difference comes from a water molecule (water 1) which connects the E106 OE1 and E117 OE1

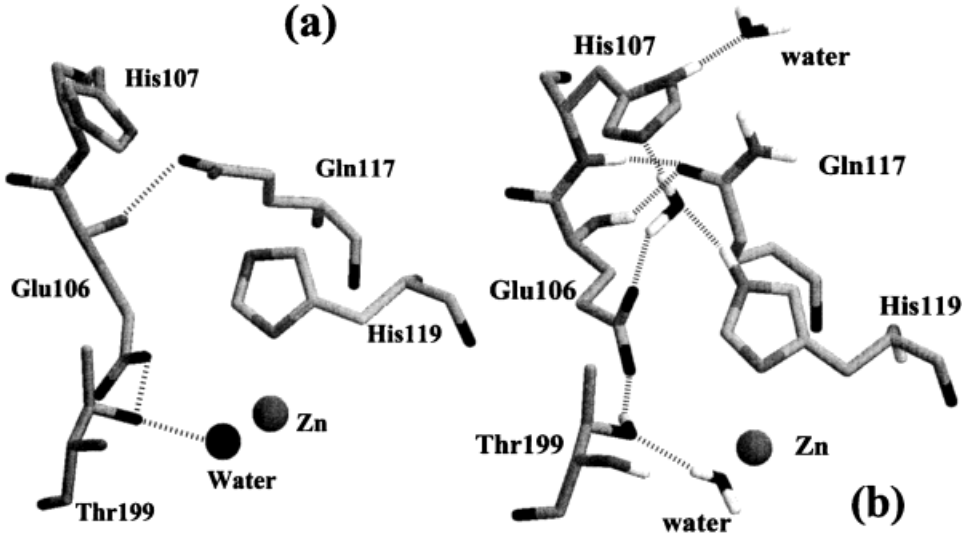

Fig. 6. **a:** The X-ray resolved structure around the residue 117 region when the structure in Figure 5(a) is mutated. It is isostructural to Figure 5(a) in the sense that no major positional change of residues is found. Hydrogen atoms are not seen in the X-ray structure. **b:** The typical picture of the E117Q mutant in MD simulations on the fully solvated enzyme. There are several structural differences from a. See text for details.

atoms through two mutual H-bonds; in the meantime, this water molecule accepts a H-bond from the H107 ND1 atom. Thus, compared with the X-ray structure, the solvated structure is more relaxed, while retaining all necessary H-bonds.

After E117 is mutated with a Gln residue, X-ray experiments[42] gave a structure which is similar to Figure 5(a) except that one OE atom is replaced by an NE atom and some H-bonds appear to have been broken [See Fig. 6(a)]. In the solvated structure [Fig. 6(b)], the situation is somewhat different: Q117 OE1 still accepts two H-bonds from the E106 and H107 backbone N atoms, but the NH_2 group is not involved in any strong H-bonding; The E106 OE1 atom now accepts one H-bond from a water molecule, which accepts an H-bond from the H119 NE2 atom. It is seen that the Gln117 residue rotates some and no longer supports His119 by a strong H-bond. Instead, a water molecule plays a similar role. This may be understood in the following way: Around the Q117 NE2 atom, there are only H-bond donors such as backbone N atoms of H107 and E106; hence the OE atom of Gln117 turns toward them while the NH_2 group turns the opposite way. This would leave a situation with the H119 NE2 atom unsupported, which causes the water which was H-bonding with Glu106 and Glu117 in Figure 5(b) to turn and accept an H-bond from H119 NE2. Meanwhile, the E106 residue is pulled from its original position somewhat. The overall H-bond structure is expected to be less rigid because of the shifts of several residues from their wild-type CA II positions, which is confirmed in the MD simulations by the fact that the H-bond between Thr199 and the Zn-bound water is frequently broken and reformed.

In terms of the changes in catalytic activity upon mutation, there may be a number of factors that cause the drop of activity to virtually zero. First, the replacement of E117 with a neutral charge will lead to changes in the Zn^{2+} binding in the active site, which is supported by the increased Zn-His distances in the MD simulations. It was found that the distance between the Zn^{2+} ion and the H119 ND1 atom increases by $\sim$0.04 Å on average upon mutation. Given a Zn-E117 distance of around 7 Å, the attractive electrostatic interaction between the Zn^{2+} ion and E117 may be as large as 15–30 kcal/mol, even considering the charge redistribution in the Zn-ligand complex and the possible dielectric screening effects. A weakening of this interaction should decrease the zinc affinity and lead to a larger dissociation constant (K_d) for the Zn^{2+} ion, as found in experiment (cf. Table I). From experimental data on the mutants E117A and Q92E,[15] this effect on the catalytic activity may be as much as 5–10 fold.

Another effect that may contribute to the increase of K_d is the H-bond of H119 with the water molecule as shown in Figure 6(b). This H-bond is expected to be much weaker than that of the Glu117 OE atom in wild-type CA II because of electrostatic and geometric considerations, which is confirmed in the MD simulations in that this H-bond is frequently broken. This in turn will affect the bonding of Zn-His119, the zinc dissociation constant, and the catalytic activity.

The motion of Thr199 can be even more significant in terms of its effect on the catalytic activity. For the protonated state of Zn-bound water, the H-bond between that water molecule and Thr199 is frequently broken; while it is constantly broken when Zn-bound water is deprotonated. Studies on T199

mutants have shown that the H-bond between hydroxyl oxygen of Thr199 and Zn-bound water/hydroxide is rather important.[15] This is understood to result from the change of H-bond formation around the Zn-bound water. The typical activity change of the Thr199 mutation is around 100–2000 fold. The frequent breakage of its H-bond with Zn-bound water could result from the shift of E106 position (cf. Fig. 6).

Another important observation involves the His64 residue. Upon mutation, the distance between the Zn^{2+} ion and the His64 NE2 atom is found to be around 11.0 Å on average in the MD simulations. This could explain why in the X-ray studies that two R(Zn-NE2) distances have been observed.[43] One is 8.1 Å, while the other is 11.9 Å. It is conceivable that the longer R(Zn-NE2) distance results from the solvated structure, while the shorter one results from the desolvated state. Both situations may be present after the process of enzyme crystallization. This conjecture was probed in the MD simulations by mutating the X-ray structure without adding water molecules, which gives an average R(Zn-NE2) distance of around 8.3 Å. Thus, in the fully solvated mutant, the proton transfer becomes very difficult indeed, which eventually may make the catalytic activity drop to essentially zero.

Yet another possible factor which may contribute to the enzyme activity is the motion of E106. X-ray studies have found that E106 is around 4 Å away from Zn-bound water/hydroxide through H-bonding with Thr199 OG1 atom in wild type CA II: the Zn-bound water/hydroxide donates a H-bond to the Thr199 OG1 atom while E106 OE1 accepts a H-bond from Thr199 OG1. This is seen in Figure 6(a). It has also been demonstrated in ab initio calculations by Liang and Lipscomb[38] that the E106 charge group COO^- is rather important to the leaving of the HCO_3^- product from the Zn^{2+} ion. With the presence of the COO^- charge group in E106, the barrier for the leaving of the HCO_3^- anion could be reduced by as much as 66 kcal/mol. This effect can be understood from the purely electrostatic interaction between the charged group and the bicarbonate ion. Although the exact leaving process of HCO_3^- from the Zn^{2+} ion is still not yet clear, the effect of E106 seems without much doubt. The replacement of E106 with the neutral residue Gln leads to a change of k_{cat}/K_M by a factor of 12.5 and k_{cat} by a factor of 900. This may suggest that the dissociation of the enzyme-product complex, $EZn - HCO_3^-$ is rate-limiting in the mutant E106Q. Thus, in light of the above argument, as E106 moves from ~4 Å to ~6.0 Å in the mutant, the effect may be as much as 20–30 kcal/mol. This number is likely to overestimate of the importance of E106 in CA II due to other compensatory structural reorganization effects, but a factor of 10–100 change in catalytic activity does not seem surprising.

To summarize, the drop in catalytic activity of the E117Q mutant is likely due to a number of factors as described above. The increase of the Zn^{2+} dissociation constant may be attributed mainly to the change of charge and the H-bond of H119 with a water molecule around the 117 residue region. It is important to emphasize the role of water molecules and the solvation effects: The motion of E106 and T199 away from the wild type CA positions in E117Q mutant leads to a change in the H-bond formation around the active site and pushes His64 away from the active site. Without water molecules in the active site, the His64 residue was found to be rather stable with an "inward" conformation. Moreover, the involvement of the water molecule H-bonding with E106 and H107 seems to play a role in the drop of activity in the E117Q variant.

The hydrogen bonding situation for mutant E117A was examined in detail as well. Here, three water molecules were found to be around the 117 residue region. Two of them, which fill the space of the E117 side chains, form hydrogen bonds with the H119 NE2 atom, while the third accepts an H-bond from the backbone E106 N atom frequently. Since no charge group is present in A117, the situation for electrostatic interactions is better than in the E117Q mutant: there is no unfavorable interaction such as the one between the Q117 NH_2 group and the H107 backbone N and side ring ND atoms.

Mutation of Thr199

In wild type CA II, Zn-bound water/hydroxide donates a hydrogen bond to Thr199 (cf. Fig. 6). Thus it seems that Thr199 would play a similar role to the indirect ligands, such as E117 and Q92. However, this does not seem to be the case. In general, mutation of Thr199 leads to a much more drastic change in catalytic power than other indirect ligand mutations.[22,26,27] Upon mutation, a decrease of 1000- to more than 5000-fold in k_{cat}/K_M is observed, while for the case of E117 and Q92 mutations, only a factor of 10 was observed, except the extreme case of E117Q which may be complicated by a number of factors as discussed previously. Thus, there must be other factors that can account for the significant consequences of the Thr199 mutations.

Three variants T199E, T199D, and T199C were prepared in the present work, and MD simulations were then performed. A structure of the T199E variant in the MD simulations is shown in Figure 7. Here it is observed that E199 directly coordinates with the Zn^{2+} ion as a fifth ligand, while there are two water molecules H-bonding with the CO_2^- group. The Zn-bound water donates an H-bond to the CO_2^- group most of the time. This structure agrees with the X-ray studies[27] in that one OE atom in CO_2^- is

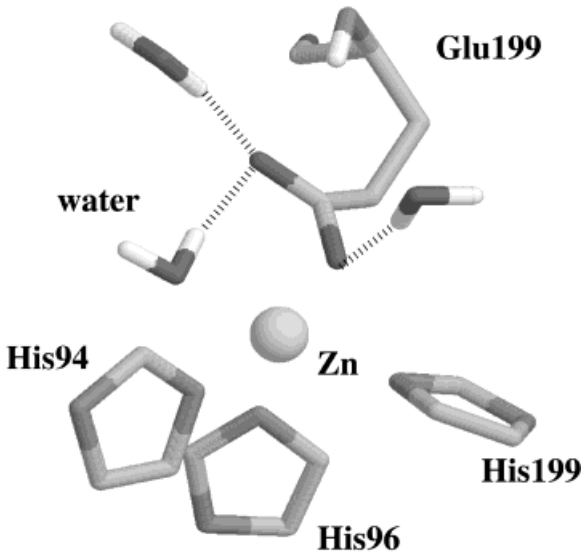

Fig. 7. The typical picture of mutant T199E found in the present MD simulations. Here E199 side chain is found to coordinate with the Zn^{2+} ion, which makes the zinc dissociation more difficult.

close to the Zn^{2+} ion (2.19 Å), and another OE is 3.89 Å away. However, the Zn-bound water is not observed in the X-ray structure, which may be due to the factor of crystallization. This resulting structure (Fig. 7) offers a possible explanation of why the zinc dissociation is decreased by a factor of 200, since the association of CO_2^- with the Zn^{2+} ion makes it more difficult for the water molecules to take position around the Zn^{2+} ion due to the more rigidly formed structure around the region, which is stabilized by the full negative charge on the CO_2^- group. Moreover, introduction of a CO_2^- group close to the Zn-bound water will make the proton transfer more difficult. As can be seen from our previous ab initio studies,[29] such a negative charged group CO_2^- is expected to increase the forward proton transfer barrier more effectively than an H-bonded water molecule. In the latter case, an increase of barrier by ~10–15 kcal/mol was found.[29]

As the side chain of E199 is decreased by a CH2 unit, one obtains D199. The typical picture of this mutant found in the MD simulations is presented in Figure 8(a). It is observed that a water molecule stays in between Glu106 and Asp199, which gives a favorable situation for electrostatic interactions. In the meantime, the Zn-bound water donates an H-bond to the Glu106 OE2 atom, with the overall structure showing a 4-fold coordinated $Zn^{2+}(His)_3(H_2O)$ complex. This offers an explanation as to why the zinc dissociation constant was not affected by the mutation. One major difference between wild type CA II and this mutated variant is again the negative charge on the CO_2^- group. Here both Glu106 and Asp199 CO_2^- groups are expected to make contributions in increasing the forward proton transfer barrier. As can be seen from Figure 8, the proton transfer from Zn-bound water (1) to water 3 will be affected by the negative charged CO_2^- groups, especially the one in Glu106, which resides in the opposite direction of forward proton transfer. Thus, a decrease of k_{cat}/K_M from 110 to 0.04 (in units of $\mu M^{-1}s^{-1}$) upon mutation is perhaps not surprising.

It should be mentioned that the X-ray experiments[44] on mutant T199D gave a somewhat different structure where the D199 residue coordinates directly with the Zn^{2+} ion as shown in Figure 8(b). This seems to present a difficulty in explaining the zinc dissociation constant, since the Zn^{2+} ion is expected to dissociate even less than the case of T199E if the X-ray structure [Fig. 8(b)] persists in solution. As the activity experiment exhibited the opposite trend,[26] it suggests that the T199D mutant undergoes a structural change as the enzyme is solvated as was found in the present MD study.

For the case of T199C (Fig. 9) with a neutral Cys side chain, it diffuses away from the Zn^{2+} ion and Zn-bound water, to as far as 5–7 Å. Its former position is then filled quickly by water molecules. There can be four water molecules H-bonding with Glu106 OE atoms in the MD simulations as shown in Figure 9. Here the Zn-bound water (1) and another water molecule (2) donate two H-bonds to OE1, while two others (3 and 4) donate two H-bonds to OE2. The water molecules 2, 3, and 4 exchange positions with other water molecules frequently and lead to more fluctuations in the region. In this case, again, the decrease of k_{cat}/K_M could be the result of the Glu106 position shift, which gets much closer to the Zn-bound water.

To be consistent with the X-ray and mutation experiments, mutant T199C with a negatively charged side chain was also studied. The starting structure was taken to be close to what is found in the X-ray study,[27] where the C199 side chain coordinates directly with the Zn^{2+} ion. Interestingly, the resulting structure was found to be similar to that of T199D, where the C199 side chain is solvated by two water molecules. Again, this difference may be attributed to the involvement of water molecules in the fully solvated structure: it is conceivable that if water molecules leave the active site in the process of crystallization, C199 could relax back to positions which were occupied by water molecules. With the Glu106 residue shifting closer to the Zn-bound water as a result of the solvation of the C199 side chain, k_{cat}/K_M may decrease dramatically.

In summary, the effect of Thr199 mutations studied in the present work comes mainly from the change of coordination of the Zn^{2+} ion and a different electrostatic environment due to the involvement of charged residues, especially the Glu106 CO_2^- group and the mutated residue side chain. As a result, the water formation around the active site is also af-

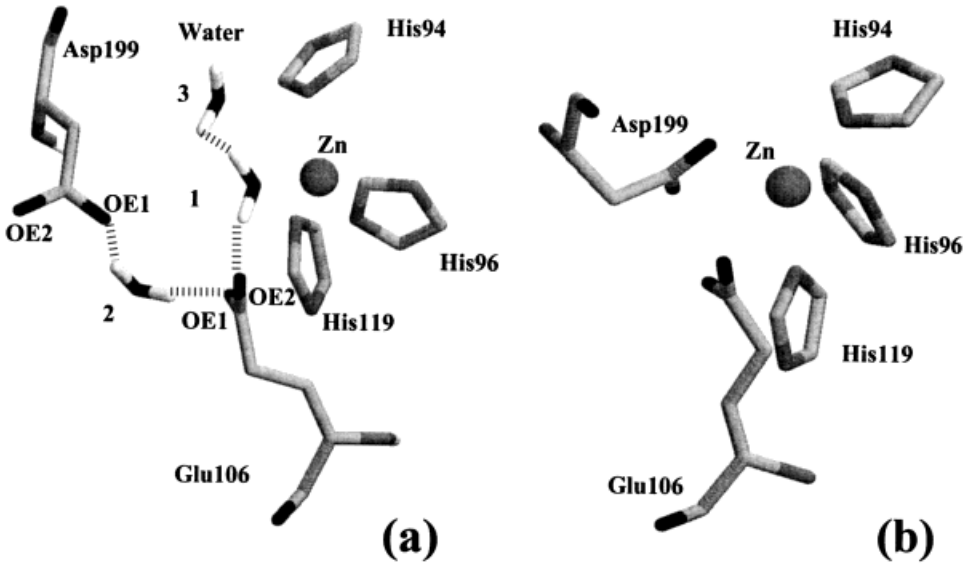

Fig. 8. The same as Figure 7 for mutant T199D.

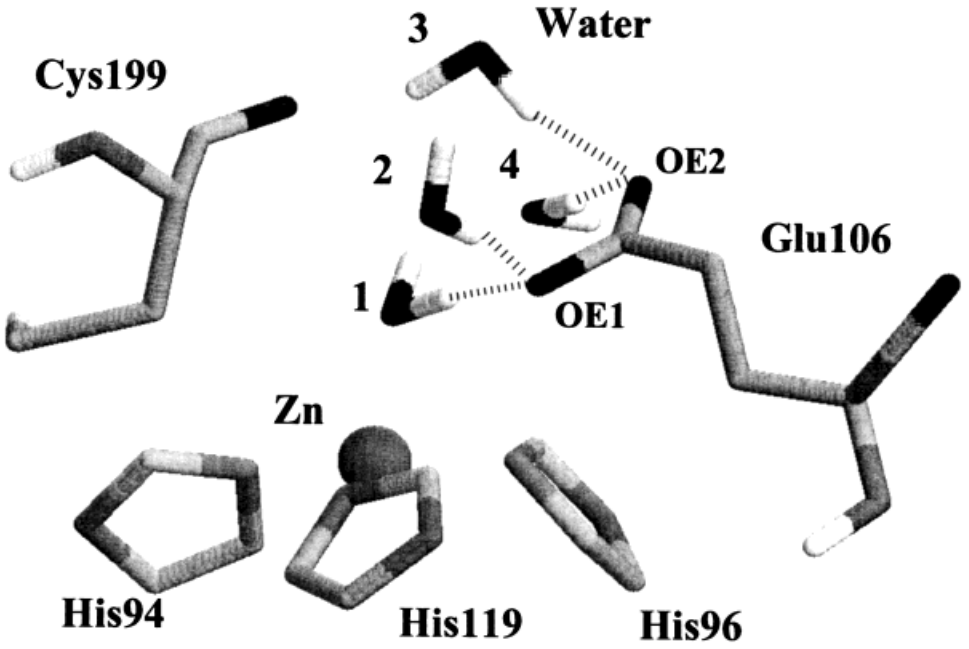

Fig. 9. The same as Figure 7 for mutant T199C with a neutral Cys side chain. Here C199 diffuses away, while Glu106 comes close to the Zn-bound water. Frequently, the H-bonds in dotted lines were found to break and reform, and the water molecules 2, 3, and 4 exchange positions with other water molecules.

fected, which may or may not have profound consequences on the catalytic activity. However, from the studies of the ligation and the position shifts of the nearby residues, it seems that the change of catalytic activity and zinc dissociation constant can be understood reasonably well. As these features are more directly involved in the catalytic process, their effects can be more profound than the indirect ligands, such as residues at the 92 and 117 positions.

CONCLUSIONS

In the present study, we have developed a model for the CA II active site by fitting force constants and

ab initio water affinities of the $Zn^{2+}(Im)_3$ complex. An application of this model in MD studies has provided new insight into various experimental findings and the role of solvation.

Through a detailed analysis of the angular interaction among the His-ligands and Zn-bound water, it was concluded that the Zn^{2+} ion is dominantly 4-fold coordinated. This result is consistent with X-ray studies. It is found that a transient 5-fold coordination involving a second water molecule can also occur.

The conformation of His64, as described by the distance between the Zn^{2+} ion and the His64 NE2, is sensitive to the protonation state of the Zn-bound water and His64. Despite some difference between the X-ray structures and the present simulations in the doubly deprotonated state, the MD result helps interpret the experimental results by Nair et al.[3] The involvement of water molecules and the H-bond formation around the active site is expected to be crucial, which was also suggested by Thr200 mutation studies.[21]

The MD studies on the transient water bridge structures relevant to the proton transfer mechanism in CA II reveal that a $2 \sim 3$ kcal/mol free energy barrier is likely to be involved. Combining these results with our previous ab initio calculations of the proton transfer barrier,[29] it is suggested that the proposed proton transfer mechanism from Zn-bound water to His64 NE2 through a water shuttle is operational. It was also found that one cannot exclude the possible existence of a single water bridge between the Zn-bound water and His64, which may give a significant contribution to the proton transfer process.

The computational mutation experiments are furthermore helpful in interpreting the dramatic change of the catalytic activity and zinc dissociation constant of E117Q. Indeed, it was shown that the involvement of water molecules seems crucial for the explanation of the experimental facts. Mutations on Thr199 can change the coordinations of the Zn^{2+} ion, modify the electrostatic interactions around the Zn^{2+} ion, and cause H-bond formation changes around the active site. All these may lead to the changes in the catalytic activity.

In conclusion, an explicit treatment of water molecules in the MD simulations of CA II and its mutants appears to be crucial for an understanding of its catalytic activity. These MD results, in combination with the X-ray studies, have helped to provide a better picture of this important enzyme.

ACKNOWLEDGMENTS

The authors thank Professors David Christianson and David Silverman for many insightful discussions.

REFERENCES

1. Fersht, A. "Enzyme Structure and Mechanism." W.H. Freeman: New York, 1985.
2. Silverman, D.N., Lindskog, S. The catalytic mechanism of carbonic anhydrase: Implications of a rate-limiting protolysis of water. Acc. Chem. Res. 21:30–36, 1988.
3. Nair, S.K., Christianson, D.W. Unexpected pH-dependent conformation of His-64, the proton shuttle of carbonic anhydrase II. J. Am. Chem. Soc. 117:9455–9458, 1991.
4. Christianson, D.W. Structural biology of zinc. Adv. Protein Chem. 42:281–355, 1991.
5. Lesburg, C.A., Christianson, D.W. X-ray crystallographic studies of engineered hydrogen bond networks in a protein-zinc binding site. J. Am. Chem. Soc. 117:6838–6844, 1995.
6. Eriksson, A.E., Jones, A.T., Liljas, A. Refined structure of human carbonic anhydrase II at 2.0 Å resolution. Proteins 4:274–282, 1988.
7. Liljas, A., Kannan, K.K., Bergsten, P.-C., Waara, I. et al. Crystal structure of human carbonic anhydrase. C. Nature 235:131–137, 1972.
8. Kannan, K.K., Ramanadham, M., Jones, T.A. Structure, refinement, and function of carbonic anhydrase isozymes: Refinement of human carbonic anhydrase I. Ann. N.Y. Acad. Sci. 429:49–60, 1984.
9. Henderson, L.E., Hendriksson, D., Nyman, P.O. Primary structure of human carbonic anhydrase. J. Biol. Chem. 251:5457–5463, 1976.
10. Kiefer, L.L., Fierke, C.A. Functional characterization of human carbonic anhydrase II variants with altered zinc binding sites. Biochemistry 33:15233–15240, 1994.
11. Ippolito, J.A., Christianson, D.W. Structural consequences of redesigning a protein-zinc binding site. Biochemistry 33:15241–15249, 1994.
12. Merz, K.M., Jr. CO_2 binding to human carbonic anhydrase II. J. Am. Chem. Soc. 113:406–411, 1991.
13. Hoops, S.C., Anderson, K.W., Merz, K.M., Jr. Force field design for metalloproteins. J. Am. Chem. Soc. 113:8262–8270, 1991.
14. Lindskog, S., Engberg, P., Forsman, C. et al. Kinetics and mechanism of carbonic anhydrase isoenzymes. Ann. N. Y. Acad. Sci. 429:61–75, 1984.
15. Christianson, D.W., Fierke, C.A. Carbonic anhydrase: Evolution of the zinc binding site by nature and by design. Acc. Chem. Res. 29:331–339, 1996.
16. Tu, C.K., Silverman, D.N., Forsman, C., Jonsson, B.-H., Lindskog, S. Role of histidine 64 in the catalytic mechanism of human carbonic anhydrase II studies with a site-specific mutant. Biochemistry 28:7913–7918, 1989.
17. Pocker, Y., Bjorkquist, D.W. Comparative studies of Bovine carbonic anhydrase in H_2O and D_2O. Stopped-flow studies on the kinetics of interconversion of CO_2 and HCO_3^-. Biochemistry 16:5698–5707, 1977.
18. Silverman, D.N., Tu, C.K., Lindskog, S., Wynns, G.C. Rate of exchange of water from the active site of human carbonic anhydrase C. J. Am. Chem. Soc. 101:6734–6744, 1979.
19. Silverman, D.N., Tu, C.K., Chen, X., Tanhouser, S.M., Kresge, A.J., Laipis, P.J. Rate-equilibria relationships in intramolecular proton transfer in human carbonic anhydrase III. Biochemistry 32:10757–10762, 1993.
20. Ghannam, A.F., Tsen, W., Rowlett, R.S. Activation parameters for the carbonic anhydrase II-catalyzed hydration of CO_2. J. Biol. Chem. 261:1164–1169, 1986.
21. Krebs, J.F., Fierke, C.A., Alexander, R.S., Christianson, D.W. Conformational mobility of His-64 in the Thr200-Ser mutant of human carbonic anhydrase II. Biochemistry 30:9153–9160, 1991.
22. Kiefer, L.L., Paterno, S.A., Fierke, C.A. Hydrogen bond network in the metal binding site of carbonic anhydrase enhances zinc affinity and catalytic efficiency. J. Am. Chem. Soc. 117:6831–6837, 1995.
23. Steiner, H., Jonsson, B.H., Lindskog, S. The catalytic mechanism of carbonic anhydrase. Eur. J. Biochem. 59:253–259, 1975.

24. Heck, R.W., Boriack-Sjodin, P.A., Qian, M. et al. Structure-based design of an intramolecular proton transfer site in murine carbonic anhydrase V. Biochemistry 35:11605–11611, 1996.
25. Christianson, D.W. Structural aspects of divergent proton translocation trajectories in carbonic anhydrases II and V. The Rigaku Journal 13:8–15, 1996.
26. Kiefer, L.L., Krebs, J.F., Paterno, S.A., Fierke, C.A. Engineering a cysteine ligand into the zinc binding site of human carbonic anhydrase II. Biochemistry 32:9896–9900, 1993.
27. Ippolito, J.A., Christianson, D.W. Structure of an engineered His_3Cys zinc binding site in human carbonic anhydrase II. Biochemistry 32:9901–9905, 1993.
28. Hartsough, D.S., Merz, K.M., Jr. Dynamic force field models: Molecular dynamics simulations of human carbonic anhydrase II using a quantum mechanical/molecular mechanical coupled potential. J. Phys. Chem. 99:11266–11275, 1995.
29. Lu, D., Voth, G.A. Proton transfer in the enzyme carbonic anhydrase: An *ab initio* study. J. Am. Chem. Soc. 120:4006–4014, 1998.
30. Besler, B.H., Merz, K.M., Jr., Kollman, P.A. Atomic charges derived from semiempirical methods. J. Comp. Chem. 11:431–439, 1990.
31. Singh, U.C., Kollman, P.A. An approach to computing electrostatic charges for molecules. J. Comp. Chem. 5:129–145, 1984.
32. Brooks, B.R., Bruccoleri, R.E., Olafson, B.D., States, D.J., Swaminathan, S., Karplus, M. CHARMM: A program for macromolecular energy minimization and dynamics calculations. J. Comp. Chem. 4:187–217, 1983.
33. Reiher, W.E., III. "Theoretical Studies of Hydrogen Bonding," Cambridge, MA: Harvard University Press, 1985.
34. Berendsen, H.J.C., Van Gunsteren, W.F., Zwinderman, H.R.J., Guertsen, R.G. Simulations of proteins in water. Ann. N.Y. Acad. Sci. 482:269–286, 1986.
35. Stote, R.H., States, D.J., Karplus, M. On the treatment of electrostatic interactions in biomolecular simulation. J. Chim. Phys. 88:2419–2433, 1991.
36. Stote, R.H., Karplus, M. Zinc binding in proteins and solution: A simple but accurate nonbonded representation. Proteins 23:12–31, 1995.
37. Liang, J., Lipscomb, W.N. Theoretical study of the uncatalyzed hydration of carbon dioxide in the gas phase. J. Am. Chem. Soc. 108:5051–5058, 1986.
38. Liang, J., Lipscomb, W.N. Theoretical study of carbonic anhydrase-catalyzed hydration of CO_2: A brief review. Int. J. Quan. Chem. 36:299–312, 1989.
39. Vedani, A., Huhta, D.W. A new force field for modeling metalloproteins. J. Am. Chem. Soc. 112:4759–4767, 1990.
40. Hakansson, K., Carlsson, M., Svensson, A., Liljas, A. Structure of native and apo carbonic anhydrase II and structure of some of its anion-ligand complexes. J. Mol. Biol. 227:1192–1204, 1992.
41. Alexander, R.S., Kiefer, L.L., Fierke, C.A., Christianson, D.W. Engineering the zinc binding site of human carbonic anhydrase II: Structure of the HIS-94 → CYS apoenzyme in a new crystalline form. Biochemistry 32:1510, 1993.
42. Huang, C.-c, Lesburg, C.A., Kiefer, L.L., Fierke, C.A., Christianson, D.W. Reversal of the hydrogen bond to zinc ligand Histidine-119 dramatically diminishes catalysis and enhance metal equilibration kinetics in carbonic anhydrase II. Biochemistry 35:3439–3446, 1996.
43. Ippolito, J.A., Baird, T.T., McGee, S.A., Christianson, D.W., Fierke, C.A. Structure-assisted redesign of a protein zinc binding site with femtomolar affinity. Proc. Natl. Acad. Sci. U.S.A. 92:5017–5021, 1995.